International Conference on "Cement – Based Materials Tailored for a Sustainable Future"
27-29 May 2021 – Istanbul / TURKEY

Towards tailored cement-based materials with ground calcium carbonates

E. Denarié[1]*, L. Sofia[2], P. Gonnon[3]

[1]Division of Maintenance and Safety of Structures (MCS-ENAC), École Polytechnique Fédérale de Lausanne (EPFL), GC A3 398, Station 18, CH-1015 Lausanne, Switzerland, emmanuel.denarie@epfl.ch,*corresponding author

[2]Construction Materials Laboratory (LMC-STI), École Polytechnique Fédérale de Lausanne (EPFL), MX G 240, Station 12, CH-1015 Lausanne, Switzerland, lionel.sofia@epfl.ch

[3]OMYA International AG, P.O. Box 335, CH-4665 Oftringen, Switzerland, pascal.gonnon@omya.com

Abstract

Proportioning the dosage of Ground Calcium Carbonates (GCC) in cementitious materials, beyond current normative levels, is one of the most promising ways towards sustainability of mortar and concrete technology. Performance parameters such as the water/binder ratio do not represent the very significant benefits in terms of mechanical performances, of clinker replacement by GCC in mixes with water/cement ratios in the range of that for normal concretes used in construction (0.4 to 0.6). Alternative parameters such as the water/fines ratio proved to be reliable indicator of performances for Ultra High-Performance Fiber Reinforced Concretes. This concept needs to be further extended to normal concretes, on a scientific basis. With this aim in view, mortar mixes with a similar water/cement ratio of 0.5 and progressive replacement of sand by GCC with water/fines ratios as low as 0.2 were studied. The packing density of the cement and GCC was determined by means of wet packing measurements using the mixing power method. The Compressible Interaction Packing Model from Fennis was generalized to multiple polydisperse components and used to predict the packing density of the mixes. The rheology at fresh state of the mixes was put into perspective with the packing density, water film thickness and sand packing factor to define reliable indicators of performances at fresh states. Finally, the compressive strength of the mixes at 1 and 28 days was related to the efficiency coefficient of the GCC used.

Keywords: *GCC, water/fines, packing, water film thickness, volume of paste.*

1 Introduction

The relevance of the water/cement or water binder ratio as a unique indicator of performance has to be questioned to progress in the optimization of the use of Ground Calcium Carbonates (GCC) in cementitious materials, beyond current normative levels. This needs to be done both with respect to the fresh state behavior of the mixes and the effect on the mechanical performances (compressive strength). GCC can be used as mineral admixtures to improve the packing vs specific surface performance of the powder mix to free voids water and increase workability, for the same water dosage. However, the paste content of the mix also has to be taken into consideration as shown by (Fennis, 2011; Li & Kwan, 2013). At fresh state, both the water film thickness and packing density of inclusions like sand aggregates or fibers play a dominant role, (Ferraris & de Larrard, 1998; Martinie, Rossi, & Roussel, 2010). In the hardened state, various authors have highlighted the relevance of the water/Fines ratio for UHPFRC mixes (Schmidt & Geisenhanslüke, 2005). (Flatt, 2004) stressed the importance of considering the relevant acting forces on the dispersion/compaction of granular mixes, to address workability, rheology of cementitious composites and action of dispersant such as superplasticizers. Globally, cementitious composites can be represented as formed of two phases : coarse inclusions such as aggregates and sand and/or fibers, and lubricating layers formed of cement/SCM paste at a coarser level and a water film at a much finer level, The water film acts at the level of inclusions with high specific surfaces typically cement grains and below (< 50 to 100 μm). The cement/SCM paste acts at the level of coarser inclusions.

The application of these principles was illustrated by a comparative study of the performances at fresh and hardened states of different mixes with one type of GCC. The cement, water and superplasticizer dosages were kept constant and the GCC dosage was increased while decreasing the sand content. The packing density of the cement and GCC was determined by means of wet packing measurements using the mixing power method. The Compressible Interaction Packing Model from Fennis was generalized to multiple polydisperse components and used to predict the packing density of the mixes.
This paper presents first the materials used, principles of the methods, and tools used. Then the experimental results at fresh state are analyzed with retrieved rheological data (yield stress) and derived models at the scale of inclusions and of the water film. Finally, the mechanical performances at two ages (1 and 28 days) of the mixes are analyzed to determine apparent activity coefficients of the GCC as a function of its dosage.

2 Bases of packing models

The Compressible Packing Model (CPM) was introduced by (De Larrard, 1999) and generalized by (Thierry Sedran, 1999) to the case of multiple polydisperse grains classes, and applied among others by (Formagini, Toledo Filho, & Fairbairn, 2005), who give a detailed description of the application of this model in the most general case, for the formulation of Ultra-High Performance Fiber reinforced Concretes (UHPFRC). This model takes into consideration on the one hand the interaction between grains of different sizes (wall and loosening effects), and on the other hand the effect of compaction energy on the achieved packing, by means of a compaction factor K. The mathematical functions of this model and their parameters describing wall and loosening effects were calibrated on laboratory test results with grains of multiple sizes, essentially sands, fine and coarse aggregates. (Fennis, 2011) further developed the CPM to achieve the CIPM (Compressible Interaction Packing Model) by modifying the mathematical functions describing wall and loosening effects in the CPM, to better represent the case of fine (< 0.125 mm) grains. The formalism of the (Schwanda, 1966) model was used with parameters and coefficients deduced from test results and numerical simulations with the HADES computational packing model (He, 2010; Stroeven, J Sluys, Guo, & Stroeven, 2006) from TU Delft. The Fennis CIPM model was applied successfully to optimize granular mixes of cement pastes, mortars and ecological concretes, with a massively reduced binder content (Fennis, 2011; Haist, Moffatt, Breiner, & Müller, 2014). (Denarié, 2016) generalized the CIPM model to the case of multiple polydisperse components (M granular components with n size classes represented by their diameter d_i or d_j)), with α_t the packing of the powder mix, $r_{k,i}$ the volumetric percentage of powder k in size class i, in the mix, p_k the volumetric dosage of powder k in the mix, $\beta_{k,i}$ the virtual packing of powder k in size class i (for an infinite compaction factor K_t), $a_{ij,c}$, $b_{ij,c}$ the functions of the loosening and wall effects, d_c, w_a et C_a the parameters of the loosening effect function and w_b, C_b the parameters of the wall effect function, equations (1) to (3). The parameters of the loosening and wall effect functions proposed by Fennis are d_c=25 µm, w_a=1, C_a=1.5, w_b=1, C_b=0.2.

$$K_t = \sum_{i=1}^{n} \frac{\sum_{k=1}^{M} \frac{\varphi_{k,i}}{\beta_{k,i}}}{\sum_{k=1}^{M} \varphi^*_{k,i} / \beta_{k,i} - \sum_{k=1}^{M} \varphi_{k,i} / \beta_{k,i}} \tag{1}$$

$$\varphi^*_{k,i} = \beta_{k,i} \cdot \mathrm{p}_k \cdot \left[1 - \left[\sum_{j=1}^{i-1} [1 - b_{ij,c}(1 - 1/\beta_{k,j})] \cdot \alpha_t \cdot r_{k,j} + \sum_{j=i+1}^{n} a_{ij,c} \cdot \alpha_t \cdot r_{k,j} / \beta_{k,j} \right] \right] \tag{2}$$
$$= \beta_i \cdot \mathrm{p}_k \cdot \left[1 - \lambda_{k,i} \right]$$

$$\varphi_{k,i} = p_k \cdot r_{k,i} \cdot \alpha_t \tag{3}$$

The loosening and wall functions are identical to those proposed by Fennis, equations (4) and (5). This model can fully represent all interactions between different granular components with different size classes. It has been used successfully to optimize UHPFRC mixes (Hajiesmaeili & Denarié, 2018).

$$a_{ij,c} = \begin{cases} 1 - \dfrac{\log_{10}(d_i / d_j)}{w_{0,a}} & if \quad \log_{10}(d_i / d_j) < w_{0,a} \\ 0 & if \quad \log_{10}(d_i / d_j) \geq w_{0,a} \end{cases} \qquad w_{0,a} = \begin{cases} w_a \times C_a & if \quad d_j < d_c \\ w_a & if \quad d_j \geq d_c \end{cases} \tag{4}$$

$$b_{ij,c} = \begin{cases} 1 - \dfrac{\log_{10}(d_j / d_i)}{w_{0,b}} & if \quad \log_{10}(d_j / d_i) < w_{0,b} \\ 0 & if \quad \log_{10}(d_j / d_i) \geq w_{0,b} \end{cases} \qquad w_{0,b} = \begin{cases} w_b \times C_b & if \quad d_i < d_c \\ w_b & if \quad d_i \geq d_c \end{cases} \tag{5}$$

3 Experimental

3.1 Components

The components used in the study were: a CEM I 42,5 R HES CCB from Italcementi, two limestone fillers (GCC) from OMYA : Betocarb® HP – OG and OMYA Betocarb® UF, normalized sand from Leucate, according to EN 196-1 (specific weight of 2640 kg/m^3, 98.5 % SiO_2 and 0.2 % water absorption), and superplasticizer CHRYSO®Fluid Premia 196 (specific weight of 1055 kg/m^3, dry extract : 25.3 %). The Particle size distribution (PSD) of the powders with d_{max} < 0.125 mm was determined with a Malvern MasterSizer. The BET Specific surface of the powders (SSA) was determined with a Micromeritics TriStar II PLUS. The characteristics of the powder components are given in Table 1.

Table 1. Characteristics of the powder components.

Component	BET SSA [m^2/g]	d_{50} [µm]	$CaCO_3$ [%]	$MgCO_3$ [%]	Specific weight [kg/m^3]
CEM I 42.5 R	0.784	16.5	-	-	3130
Betocarb® HP-OG (F_1)	1.120	8.3	98.3	0.3	2700
Betocarb® UF (F_2)	5.186	2.5	98	0.42	2700

The particle size distribution of the granular components is shown on Figure 1.

3.2 Mixes

Seven different ternary mixes were investigated at fresh and hardened state, with constant weight of cement (380 g), water (190 g) and superplasticizer (3 g). The corresponding composition of the mixes per m^3 is given in Table 2. The principle of the mix design was to progressively replace sand by filler F_1, in mass, while leaving the cement, water and superplasticizer dosages constant. This induces two contradictory effects that are reflected in the workability results: increase of the paste volume and simultaneous decrease of the water film thickness, as will be shown later.

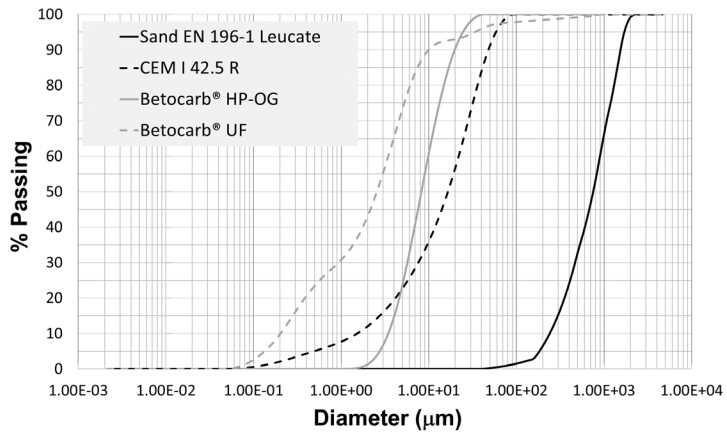

Figure 1. PSD of the granular components.

The sand content of mix T1 was 1450 g and decreased by increments of 100 g for subsequent mixes. The Filler F_1 dosage of mix T1 was 0 g and progressively increased by increments of 100 g for subsequent mixes. The air content was back calculated from the mix design for mixes T1 to T6, knowing the specific weights. For mix T7, the specific weight was not determined and an air content of 5 % was assumed based on the workability and air contents for mixes T1 and T2. The specific weight of mix T7 was determined from the assumed air content.

Table 2. Ternary mixes, composition per m^3, *: assumed.

Mix	Norm Sand [kg/m³]	Cement [kg/m³]	Filler F_1 [kg/m³]	Water [kg/m³]	W/C [-]	SP [kg/m³]	SP/(C+F_1) [%]	Specific weight [kg/m³]	Air [%]
T1	1612	422	0.0	211	0.506	3.3	0.78	2250	4
T2	1509	424	112	212	0.506	3.4	0.63	2260	3.6
T3	1442	438	231	219	0.506	3.5	0.52	2330	0.6
T4	1330	440	347	220	0.506	3.5	0.44	2340	0.4
T5	1215	440	463	220	0.506	3.5	0.39	2340	0.47
T6	1071	428	564	214	0.506	3.4	0.34	2280	3.15
T7	941	420	664	210	0.506	3.3	0.30	2239	5*

3.3 Methods

Dry packing of the normalized sand was determined as the ratio of its bulk density over its specific gravity. The bulk density was determined by weighing the mass of sand that filled a 1-liter pot, after SN EN 1097-3 (sand poured loosely without compaction). The specific gravity of the sand was measured with the pycnometer method according to ASTM C 127 and SN EN 1097-6. Wet packing of the powders was determined by means of the mixing power method from (Marquardt, 2001). A 5-liter Perrier mortar mixer (compliant to EN 196-1) was used. The mixing power was monitored and recorded with a sampling frequency of 1 s, by means of a Camille Bauer Metrawatt SA system, with an energy meter module SINEAX DM5S-0 111 1000 (with bus RS485) linked to the mixer via the electrical power supply 380 V and to a computer with software SmartCollect, via a USB port. Instead of a continuous liquid supply, an incremental addition method was used (10 ml steps). 2000 g of the powders (individual ones or binary mixes without sand) were introduced in the bowl. The liquid (water + superplasticizer) was prepared ahead so that the quantity of superplasticizer added at the supposed peak of power (guessed from the packing model) represented the desired dosage in terms of percentage mass of powders. The real-time visualization of the mixing power vs time curve helped detect the mixing power peak. The incremental addition of liquid went on until the mixing power peak was clearly passed. The packing α_t of the powder mix was calculated after equation (6)a, with ρ_{ms} the absolute specific weight of the powder (or powder mix), in kg/m³), $m_{l,pic}$ the mass of liquids added at the mixing power peak (in g), and m_p the mass of powders (in g). The dosage of superplasticizer at the mixing power peak *%SP*, in % mass of the powder mix, was calculated after the test according to equation (6)b, with $m_{l,peak}$ the mass of liquid added at the mixing power peak (in g), m_p the mass of powders (in g), m_{SP} the mass of superplasticizer in the original liquid mix (in g), m_w the mass of water in the original liquid mix (in g). The effect of the superplasticizer dosage on the wet packing of cement (partial deflocculation) was determined by the same method.

$$\alpha_t = \frac{1000}{1000 + \left(\frac{\rho_{dry,mix} \cdot m_{l,peak}}{m_p} \right)} \quad (a) \qquad \%SP = 100 \cdot \frac{m_{l,peak}}{m_p} \cdot \frac{\frac{m_{SP}}{m_w}}{1 + \frac{m_{SP}}{m_w}} \quad \text{(b)} \qquad (6)$$

All wet packing measurements were repeated three times at least. In a first step, the compaction factor *Kt* corresponding to the mixer was determined by inverse analysis of results of wet packing measurements on binary mixes, with cement and ultrafine GCC F_2. The superplasticizer dosage was 1 % of the (Cement + Filler) mass. Note that it is not possible to properly disperse GCC alone with superplasticizer, without the alkalinity provided by cement. Accordingly, mixes with 20 and 10 % of cement by vol. were the extreme cases for the measurements, from which the value at 100 % vol. of filler could be extrapolated following the method proposed by (T. Sedran, 1999). The maximum packing was achieved as expected for slightly less than 40 % vol. ultrafine Filler F_2. The best fit of the experimental packing results was obtained with the CIPM Model for a compaction factor of 12.2, similar to the value obtained by (Fennis, 2011) for mortars. In a second step, the wet packing of the coarser filler F_1 was also determined by the extrapolation to 100 % vol. of the measurements for the binary mixes with 80 and 90 % vol. Finally, a sensitivity analysis of the effect of the superplasticizer dosage on the apparent wet packing value was realized for the cement.

The workability of the mixes was determined with a mini cone for mortars (diameters 50 and 100 mm, height 150 mm). The final spread and the slump were measured. The dry bulk density of the prisms was determined after EN 1015-10. The compressive strength was determined on ½ prisms from bending tests on 40/40/160 mm prisms fabricated and tested according to EN 12390-3 : 2012 and EN 12390-5 : 2012.

3.4 Results

The specific density of the sand was 2637 kg/m^3 (average of 6 measurements) and its bulk value was 1693 kg/m^3 (average of 3 measurements) thus yielding a dry packing density of 1693/2637 = 0.642, for a compaction factor of 4.1 for loose dry packing (De Larrard, 1999). Table 3 summarizes the results of the wet packing measurements.

Table 3. Summary of wet packing measurement results (average values), compaction factor *Kt*=12.2.

Component	SP dosage [%]	Packing [-]
Cement	0.50	0.620
Cement	0.94	0.634
Cement	1.35	0.645
Cement	1.75	0.651
Filler F_1	0.90	0.680
Filler F_2	1.00	0.660

Table 4 gives the results of all measurements together with the calculated packing for the ternary mixes according to the generalized CIPM, for a compaction factor *Kt*=12.2, using the packing density of the individual components given in Table 3. As already mentioned, the superplasticizer dosage in percent mass of cement plus filler F_1 was not constant for all mixes. Accordingly, the packing density of the cement and filler was adapted for the model, based on the trend observed for the cement (see Table 3). The water film thickness *wft* was calculated from the packing density and the cumulative surface of the dry components of the mix according to equations (7) with W_t, the total quantity of water in the mix (added water + part of superplasticizer), W_{added} the added water, W_{SP} the water contained in the superplasticizer, W_v the water that fills voids in the dry mix, W_f the additional water contributing to the water film, all in liter/m^3, SSA_i the specific surface of dry component *i* in m^2/kg, M_i the mass in kg/m^3 of component *i* in the mix and *A* the air content in the mix in liter/m^3 (Krell, 1985). It was assumed that both air and voids water fill the voids complementary to the packing of the dry components. The ratio of volume of sand ϕ_s in the mix over packing of the sand ϕ^*_s, defined as the Sand Packing Factor (SPF) was calculated according to equation (8). The yield stress of the mixes was back calculated according to two models of literature (Kokado & Miyagawa, 1999; Roussel & Coussot, 2005; Roussel, Stefani, & Leroy, 2005; Tanigawa & Mori, 1985), based on the measurements at fresh state, equations (9) with ρ the specific weight of the fresh mix, *g* the acceleration due to gravity, h_0 the height of the slump cone, *s* the measured slump value, *R* radius of final spread, V_0 the volume of fresh material in the cone. For limited spread, with dominant slump, (Mixes T1 and T7), values from model 1 were selected. For Mixes T2 to T6, with slump values close to the height of the test cone and for which spread dominates, values from model 2 were selected. One can note the good correspondence of the values obtained from the two models for the intermediate case of mix T1. Mixes T1 and to a lesser extent T2 exhibited bleeding and as such, the values of the calculated wft are upper bounds. Mix T7 was stiff due to the lack of water film thickness, even if the paste content was the highest.

$$W_f = W_t - W_v = W_t - 1000 \cdot (1 - \alpha_t) - A$$
$$wft = W_f / (\sum_{1=1}^{n} SSA_i \cdot M_i) \quad (7)$$

$$SPF = \frac{\phi_s}{\phi_s^*} \quad (8)$$

$$\tau_1 = \frac{\rho g (h_0 - s)}{\sqrt{3}} \quad \text{(model 1)} \qquad \tau_2 = \frac{225 \rho g}{128 \pi^2 R^5} V_0^2 \quad \text{(model 2)} \quad (9)$$

Table 4. Ternary mixes, workability, packing, wft, paste volume, Sand Packing Factor (SPF), yield stress (model 1, model 2 and selected) and average compressive strength at 1 and 28 days.

Mix	Spread [mm]	Slump [mm]	Packing α_t [-]	wft [nm]	Paste volume [%]	SPF [-]	τ_1 Slump [Pa]	τ_2 Spread [Pa]	τ Selected [Pa]	$f_{c,1}$ [MPa]	$f_{c,28}$ [MPa]
T1	145	80	0.873	374.0	38.9	0.952	912	1088	912	12	39
T2	235	130	0.883	288.0	42.9	0.889	261	97	97	14	39
T3	370	150	0.874	167.0	45.4	0.850	0	10	10	21	50
T4	405	150	0.858	114.0	49.6	0.785	0	6	6	23	61
T5	430	150	0.839	76.0	54.0	0.717	0	5	5	25	64
T6	265	140	0.817	67.0	59.4	0.632	130	53	53	25	58
T7	100	20	0.793	52.0	64.4	0.555	1693	6972	1693	ND	ND

4 Analysis of results at fresh state

Figure 2a) presents the effect of the water film thickness on the logarithm of the shear stress for mixes T5, T6, T7 where the effect of the wft dominates, and for data from (Kwan, Fung, & Wong, 2010) on self-compacting mortars. For both sets of data a linear trend is clear in the Ln(shear stress) representation, as already shown by (Kwan et al., 2010) for their data. The three points for mixes T5, T6, T7 of the present study show a steep decrease with the increase of the wft between 50 and 80 nm. Results for mixes T1, T2, T3, T4 are much more influenced by the paste volume, and thus the SPF. The data of (Kwan et al., 2010) fits well on a much milder decrease with wft, from 50 nm on. On the basis of these sets of data, a new model is proposed to consider the effects of both paste volume i.e. SPF, and wft. The model is formed of two parts, equations (10). Part 1 is based on the (Quemada, 1977) model originally applied to the viscosity of suspensions. The second part takes into consideration two domains of influence of the wft on the basis of the data shown on Figure 2a), with a threshold value wft*. The full set of results of the present study is shown on Figure 2b), together with the predictions of the original Quemada model not considering the effect of the wft and of the new model that represents well the measurement data. Predictions of the new model are also shown in form of iso wft lines for varying SPF values. The threshold value wft* could be related to domains of action of the forces acting on the fresh mix. Below wft*, dispersion forces act, with a steep decrease with distance. Above wft*, the pure lubrification of the additional film water dominates.

$$\tau = \begin{cases} \tau_0 \cdot (1-\dfrac{\phi_s}{\phi_s^*})^{-2} + \mathrm{e}^{(a-b\cdot wft)} & if \quad wft < wft^* \quad a = 20.146 \quad b = 0.2434 \\ \tau_0 \cdot (1-\dfrac{\phi_s}{\phi_s^*})^{-2} + \mathrm{e}^{(c-d\cdot wft)} & if \quad wft \geq wft^* \quad c = 1.7317 \quad d = 0.0056 \\ wft^* = 80\,nm & \tau_0 = 0.5\,Pa \end{cases} \tag{10}$$

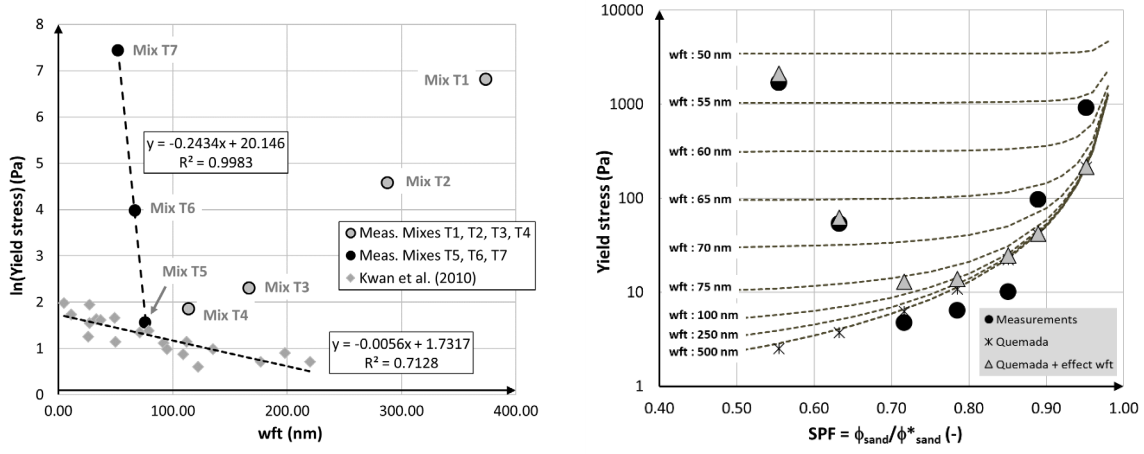

a) **b)**

Figure 2. a) effect of water film thickness on shear stress, data for mixes T1 to T7 and from (Kwan et al., 2010), b) effect of sand packing factor and water film thickness for mixes T1 to T7, measurement data and models.

5 Analysis of mechanical properties

(Chanvillard & Basuyaux, 1996)adapted the Féret model to the case of sand concretes with limestone fillers. This model was used to fit the data obtained in the present study according to equation (11) with $f_{cm,avg}$: the average compressive strength of the mortar, $k_{g,f}$: the Féret coefficient, $f_{ccem,\ avg}$: the average compressive strength of the normal mortar for the cement used, v_W : the volume of water in the mix, v_{Wsp} : the volume of water in the plasticizer used in the mix, v_{Air} : the volume of air in the mix, v_{Wabsor} : the volume of water absorbed by the sand, v_c : the volume of cement in the mix, F/C the mass ratio of filler over cement in the mix, k_{GCC} the activity coefficient of the filler.

$$f_{cm,avg} = k_{g,f} f_{ccem,avg} \frac{1}{\left(1+\frac{v_W + v_{W_{sp}} + v_{Air} - v_{W_{absor}}}{v_c(1+\frac{F}{C}k_{gcc})}\right)^2} \quad (11)$$

The average compressive strength of the cement $f_{ccem,\ avg}$ is 17 MPa at 1 day and 58 MPa at 28 days, according to the data of the producer. The Féret coefficient that best fitted the test results was 5.8 at 1 day and 5.3 at 28 days. Figure 3a) shows the evolution of the activity coefficient of the filler k_{GCC} at 1 and 28 days, as a function of the filler dosage F/C in % mass of cement, together with data at 28 days, from (Chanvillard & Basuyaux, 1996). The results of the present study at 28 days correspond well with the later, especially in terms of the value at stabilization of k_{GCC}. The significantly higher values of the activity coefficient at 28 days in the present study could be related to the mineralogy of the filler and its size distribution. At 1 day, a much higher activity of the filler is noted, that can be explained by the higher availability of aluminates, potentially reactive with limestone fillers, that are quickly consumed after 1 day (Bonavetti, Rahhal, & Irassar, 2001). Figure 3b) illustrates the trends for the effective dosage of GGC.

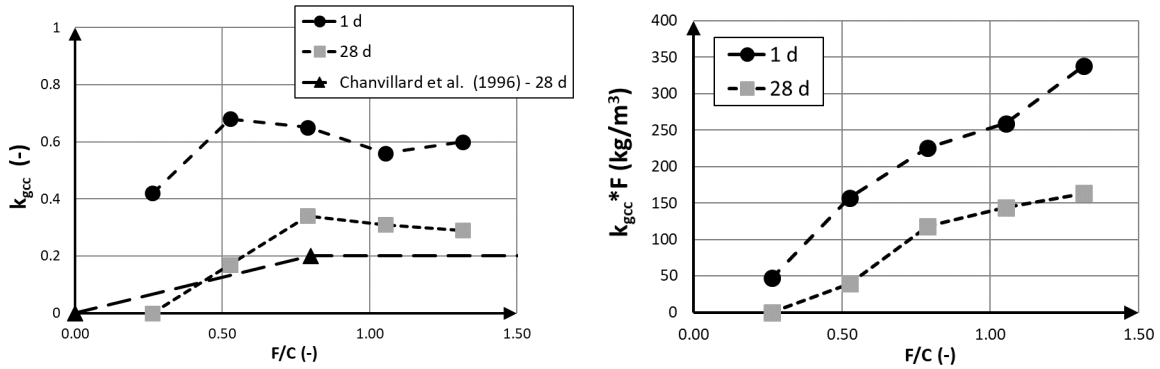

Figure 3. a) effect of the filler dosage in mass % of cement on the activity coefficient at 1 and 28 days, with data at 28 days from (Chanvillard & Basuyaux, 1996), b) effective dosage of filler at 1 and 28 days, as a function of the filler dosage in % mass cement.

6 Conclusions

- Mortar mixes with varying dosages of GCC were tested at fresh and hardened state with dosages up to 158 % of the cement mass. The composition of the mixes covered a wide range of paste volumes and water film thicknesses, as well as rheological responses at fresh state.
- Wet packing measurements combined with an improved packing model helped determine the packing of all mixes and the water film thicknesses.
- The yield stress of all mixes could be back calculated from slump or spread values. A new model was proposed to relate the yield stress to the Sand Packing Factor and water film thickness of the mixes. This model showed a very good correspondence with the obtained test results.
- The activity coefficient of the GCC could be determined at 1 and 28 days, as a function of the GCC dosage, on the basis of the Féret formula. The obtained values highlight the high potential of limestone fillers to contribute to the compressive strength of cementitious materials, beyond current normative limits.

7 References

Bonavetti, V. L., Rahhal, V. F., & Irassar, E. F. (2001). Studies on the carboaluminate formation in limestone filler-blended cements. *Cement and Concrete Research, 31*(6), 853-859. doi:https://doi.org/10.1016/S0008-8846(01)00491-4

Chanvillard, G., & Basuyaux, O. (1996). Une methode de formulation des bétons de sable à maniabilité et résistance fixées. *Bulletin des laboratoires des ponts et chaussées, 205*, 49-64.

De Larrard, F. (1999). *Concrete mixture proportioning: a scientific approach*: E & FN Spon.

Denarié, E. (2016). *The generalized CIPM derivation, Internal communication* MCS/EPFL.

Fennis, S. (2011). *Design of ecological concrete by particle packing optimization.* (Doctoral thesis). TU Delft,

Ferraris, C. F., & de Larrard, F. (1998). *Testing and Modeling of Fresh Concrete Rheology* Gaithersburg, MD 20899, USA.

Flatt, R. J. (2004). Dispersion forces in cement suspensions. *Cement and Concrete Research, 34*(3), 399-408. doi:10.1016/j.cemconres.2003.08.019

Formagini, S., Toledo Filho, R., & Fairbairn, E. (2005). *Mix Design, Autogenous Shrinkage, and Mechanical Characterization of UHPFRCC.* Paper presented at the International RILEM workshop on high performance fiber reinforced cementitious composites (HPFRCC) in structural applications, Honolulu, Hawaii, USA.

Haist, M., Moffatt, J. S., Breiner, R., & Müller, H. S. (2014). Entwicklungsprinzipien und technische Grenzen der Herstellung zementarmer Betone. *Beton- und Stahlbetonbau, 109*(3), 202-215. doi:10.1002/best.201300068

Hajiesmaeili, A., & Denarié, E. (2018). *Next generation UHPFRC for sustainable structural applications.* Paper presented at the DSCS 2018: 2nd International Workshop on Durability and Sustainability of Concrete Structures, ACI SP-326, Moscow, Russia.

He, H. (2010). *Computational modelling of particle packing in concrete.* (Doctoral thesis). TU Delft,

Kokado, T., & Miyagawa, T. (1999). Study on a method of obtaining rheological coefficients of high-flow concrete from slump flow test. *Doboku Gakkai Ronbunshu, Journal of Materials, Concrete Structures and Pavements of JSCE, 1999*(634), 113-129. doi:10.2208/jscej.1999.634_113

Krell, J. (1985). *Die Konsistenz von Zementleim, Mörtel und Beton und ihre zeitliche Veränderung*: Beton-Verl. D@: usseldorf.

Kwan, A., Fung, W., & Wong, H. (2010). Water film thickness, flowability and rheology of cement-sand mortar. *Advances in Cement Research, 22*(1), 3-14.

Li, L. G., & Kwan, A. K. H. (2013). Concrete mix design based on water film thickness and paste film thickness. *Cement and Concrete Composites, 39, Supplement C*, 33-42. doi:https://doi.org/10.1016/j.cemconcomp.2013.03.021

Marquardt, I. (2001). *Ein Mischungskonzept für selbstverdichtenden Beton auf der Basis der Volumenkenngrößen und Wasseransprüche der Ausgangsstoffe.* (Doctoral thesis). Rostock, Rostock, Germany. (Volume 7 - Rostocker Berichte aus dem Fachbereich Bauingenieurwesen)

Martinie, L., Rossi, P., & Roussel, N. (2010). Rheology of fiber reinforced cementitious materials: classification and prediction. *Cement and Concrete Research, 40*(2), 226-234. doi:10.1016/j.cemconres.2009.08.032

Quemada, D. (1977). Rheology of concentrated disperse systems and minimum energy dissipation principle. *Rheologica Acta, 16*(1), 82-94. doi:10.1007/BF01516932

Roussel, N., & Coussot, P. (2005). "Fifty-cent rheometer" for yield stress measurements: From slump to spreading flow. *Journal of Rheology, 49*(3), 705-718. doi:10.1122/1.1879041

Roussel, N., Stefani, C., & Leroy, R. (2005). From mini-cone test to Abrams cone test: measurement of cement-based materials yield stress using slump tests. *Cement and Concrete Research, 35*(5), 817-822. doi:https://doi.org/10.1016/j.cemconres.2004.07.032

Schmidt, M., & Geisenhanslüke, C. (2005). Optimierung der Zusammensetzung des Feinstkorns von Ultra-Hochleistungs-und von selbstverdichtendem Beton. *beton, 55*(5), 224-223.

Schwanda, F. (1966). Das rechnerische Verfahren zur Bestimmung des Hohlraumes und Zementleimanspruches von Zuschlägen und seine Bedeutung für den Spannbetonbau. *Zement und Beton, 37*(8-17), 13.

Sedran, T. (1999). Mesure de la demande en eau. In *BétonlabPro 3 Leçon N°7, "Demandes en (super)plastifiant et en eau des additions minérales"*. Nantes, France: Laboratoire Central des Ponts et Chaussées.

Sedran, T. (1999). *Rhéologie et rhéométrie des bétons. Application aux bétons autonivelants.* (Doctoral thesis). ENPC, Paris.

Stroeven, P., J Sluys, L., Guo, Z., & Stroeven, M. (2006). Virtual reality studies of concrete. *FORMA, 21*, 227-242.

Tanigawa, Y., & Mori, H. (1985). *Rheological analysis of slumping behavior of fresh concrete.* Paper presented at the 29th Japan Congress on Materials Research.